

Photocontrolled Living Anionic Polymerization of Phosphorus-Bridged [1]Ferrocenophanes: A Route to Well-Defined Polyferrocenylphosphine (PFP) Homopolymers and Block Copolymers

Sanjib K. Patra,^[a] George R. Whittell,^[a] Simone Nagiah,^[a] Cheuk-Lam Ho,^[a, b] Wai-Yeung Wong,^{*[b]} and Ian Manners^{*[a]}

Abstract: Phosphorus-bridged strained [1]ferrocenophanes $[\text{Fe}\{(\eta\text{-C}_5\text{H}_4)_2\text{P}(\text{CH}_2\text{CMe}_3)\}]$ (**2**) and $[\text{Fe}\{(\eta\text{-C}_5\text{H}_4)_2\text{P}(\text{CH}_2\text{SiMe}_3)\}]$ (**3**) with neopentyl and (trimethylsilyl)methyl substituents on phosphorus, respectively, have been synthesized and characterized. Photocontrolled living anionic ring-opening polymerization (ROP) of the known phosphorus-bridged [1]ferrocenophane $[\text{Fe}\{(\eta\text{-C}_5\text{H}_4)_2\text{P}(\text{CMe}_3)\}]$ (**1**) and the new monomers **2** and **3**, initiated by $\text{Na}[\text{C}_5\text{H}_5]$ in THF at 5 °C, yielded well-defined polyferrocenylphosphines

(PFPs), $[\text{Fe}\{(\eta\text{-C}_5\text{H}_4)_2\text{PR}\}]_n$ ($\text{R} = \text{CMe}_3$ (**4**), CH_2CMe_3 (**5**), and CH_2SiMe_3 (**6**)), with controlled molecular weights (up to ca. 60×10^3 Da) and narrow molecular weight distributions. The PFPs **4–6** were characterized by multinuclear NMR spectroscopy, DSC, and by GPC analysis of the corresponding poly(ferrocenylphosphine sulfides) obtained by

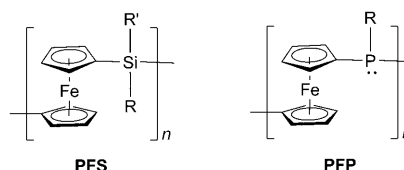
sulfurization of the phosphorus(III) centers. The living nature of the photocontrolled anionic ROP allowed the synthesis of well-defined all-organometallic PFP-*b*-PFS_F (**7a** and **7b**) (PFS_F = polyferrocenylmethyl(3,3,3-trifluoropropyl)silane) diblock copolymers through sequential monomer addition. TEM studies of the thin films of the diblock copolymer **7b** showed microphase separation to form cylindrical PFS_F domains in a PFP matrix.

Keywords: block copolymers • metallopolymers • phosphanes • photolysis • self-assembly

Introduction

Polymers containing transition metals in the main chain are of growing interest because of their intriguing physical and chemical properties and their possible applications.^[1] Over the past few decades, ring-opening polymerization (ROP) of strained metallocenophanes has attracted attention as a

route to metallopolymers.^[2] In this context, polyferrocenylsilanes (PFSs)^[3] in particular have been systematically studied. These materials have been shown to exhibit a range of



R, R' = alkyl or aryl substituent

[a] Dr. S. K. Patra, Dr. G. R. Whittell, S. Nagiah, C.-L. Ho, Prof. I. Manners
School of Chemistry, University of Bristol
Cantock's Close, Bristol, BS8 1TS (UK)
Fax: (+44) 117-929-0509
E-mail: ian.manners@bristol.ac.uk

[b] C.-L. Ho, Prof. W.-Y. Wong
Department of Chemistry, Hong Kong Baptist University
Kowloon Tong, Hong Kong (P. R. China)
Fax: (+852) 3411-7348
E-mail: rwywong@hkbu.edu.hk

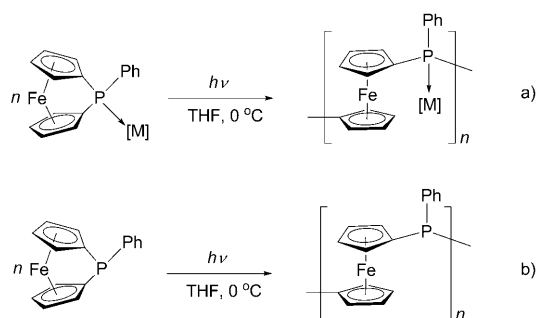
Supporting information for this article is available on the WWW under <http://dx.doi.org/10.1002/chem.200902886>. It contains GPC curves for the sulfurized PFP homopolymers **5a–e** and additional characterization data including DSC scans for the PFP homopolymers and diblock copolymers.

interesting characteristics, such as a controlled response to a redox stimulus, thereby allowing their use in photonic crystal devices and as single-chain motors,^[4] etch resistance to plasmas,^[5] high refractive indices,^[6] and to function as precursors to nanostructured magnetic ceramics^[7] and carbon nanotube growth catalysts.^[8] More recently, their ability to form crystalline, self-assembled materials has attracted growing attention.^[9]

Phosphorus-containing polymers are of considerable interest because of the variety of their applications as electroluminescent devices, sensors, biomaterials, and as catalyst supports for organic transformations.^[10] Ferrocene-based organophosphorus materials, such as polyferrocenylphosphines (PFPs)^[11] have also been the focus of several investigations. These metallopolymers also show possible applications as polymer-supported catalysts as these contain ligating phosphine centers in the main chain that should permit the introduction of additional metal fragments. The unusually high refractive index of PFPs is also a potentially interesting and useful property for photonic applications.^[6b] Furthermore, micellization of the block copolymers with PFP as one of the blocks should also permit the preparation of polymer-metal hybrid nanomaterials that may find potential applications as novel catalysts or as precursors to magnetic nanostructures.

Relative to their silicon analogues, phosphorus-bridged [1]ferrocenophanes are much less explored. The first PFP, polyferrocenylphenylphosphine, was prepared by a condensation route from $[\text{Fe}(\eta\text{-C}_5\text{H}_4\text{Li})_2]$ and PhPCl_2 in 1982.^[12] Although several polymerization routes, such as thermal^[13] and anionic ROP,^[11] have subsequently been developed to access PFPs, the synthesis of well-defined and high molecular weight PFPs still represents a considerable synthetic challenge. Living anionic polymerization initiated by organolithium reagents proceeds by cleavage of a phosphorus-cyclopentadienyl (P-Cp) bond in the monomer. The stringent experimental requirements and the presence of the strongly basic initiator and propagating center, which creates incompatibility with most functional groups, makes the development of other controlled synthetic ROP methods desirable. Another potentially versatile approach involves transition-metal-catalyzed ROP, but this is ineffective due to the poisoning of the employed catalysts by coordination to the phosphorus centers.^[14]

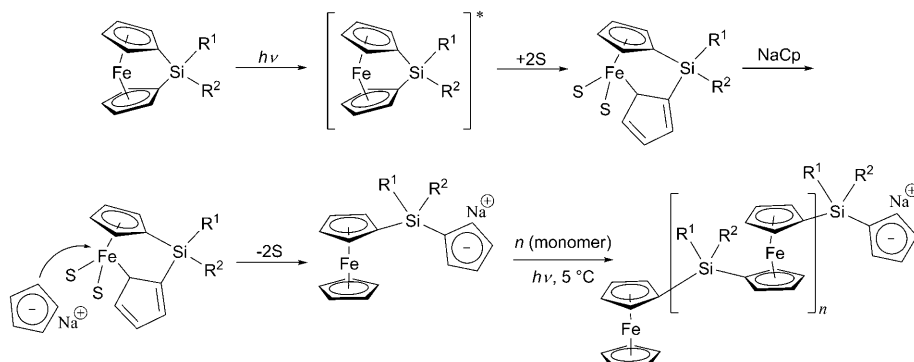
Photolytic ROP is the most recently discovered pathway to obtain well-defined high molecular weight polyferrocenes. In 2000, Miyoshi and co-workers first reported the photolytic ROP of phosphorus-bridged [1]ferrocenophane, $[\text{Fe}(\eta\text{-C}_5\text{H}_4)_2\text{PPh}]$ after complexation of the phosphorus(III) center to transition-metal fragments $[\text{M}]$ ($[\text{M}] = [\text{Mn}(\eta\text{-C}_5\text{H}_4\text{Me})(\text{CO})_2]$, $[\text{Mn}(\eta\text{-C}_5\text{H}_5)(\text{CO})_2]$, and $[\text{W}(\text{CO})_5]$).^[15] These phosphorus-bridged [1]ferrocenophane derivatives were found to undergo ROP upon UV irradiation in polar solvents, such as THF and CH_3CN , to yield PFPs in which the metal fragments ($[\text{M}]$) remained coordinated (Scheme 1a). Later, the same group reported the photolytic ROP



Scheme 1. Photolytic ROP of phosphorus-bridged [1]ferrocenophanes.^[15,16]

of $[\text{Fe}(\eta\text{-C}_5\text{H}_4)_2\text{PPh}]$ when irradiated by UV light in THF at 0 °C, through a M-Cp bond cleavage mechanism affording PFPs with a broad molecular weight distribution (Scheme 1b).^[16] In the work described, no externally added initiator was used and the polymerization was non-living with no control of molecular weight.

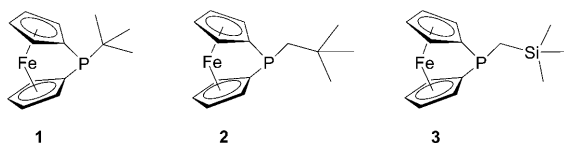
Recently, our group has shown that in the case of silicon-bridged [1]ferrocenophanes, the photopolymerization route can be transformed into a living process if a mild nucleophile, $\text{Na}[\text{C}_5\text{H}_5]$, is added as an initiator (Scheme 2). Under



Scheme 2. Mechanism for the photolytic polymerization of silicon-bridged [1]ferrocenophanes (S=solvent, for example, THF; * = photoexcited monomer).

these conditions, the polymerization can be controlled by simply “switching on” or “off” the light, allowing the sequential addition of different monomers and providing a route to well-defined block copolymers. Moreover, with a moderately basic, delocalized cyclopentadienyl (Cp) anion as the initiator and propagating site, this “soft” living polymerization method is easier to perform in practice than the conventional procedures that use organolithium initiators and also allows for the controlled and living polymerization of functional monomers containing more sensitive functionalities.^[17] We have also shown that this method can be used for the ROP of [2]dicarbaferrocenophanes, which had only previously been polymerized by using the thermal ROP method.^[18]

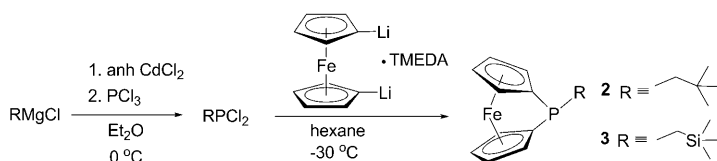
In this paper, we report the photocontrolled living anionic ROP of phosphorus-bridged [1]ferrocenophanes, $[\text{Fe}(\eta\text{-C}_5\text{H}_4)_2\text{PR}]$ **1–3**, containing alkyl substituents (CMe_3 ,



CH_2CMe_3 , and CH_2SiMe_3) on phosphorus. This affords high molecular weight homopolymers with narrow molecular weight distributions. The living nature of the photocontrolled ROP also permits access to well-defined diblock copolymers with PFSs. Preliminary studies of the thermal properties and thin film self-assembly of these diblock copolymers are also described.

Results and Discussion

Synthesis of phosphorus-bridged [1]ferrocenophanes: Phosphorus-bridged [1]ferrocenophanes were first reported in 1980 by Osborne et al.^[19] and by Seyferth and co-workers.^[12] A further significant contribution in this area was reported shortly thereafter by Cullen.^[20] The phosphorus-bridged [1]ferrocenophane **1** was prepared by following a similar procedure to that reported by Cullen and co-workers by using the commercially available *tert*-butyldichlorophosphine.^[20] The precursors, alkylidichlorophosphines (RPCl_2) with neopentyl (CH_2CMe_3) and (trimethylsilyl)methyl (CH_2SiMe_3) groups, were synthesized in good yields by the reaction of phosphorus trichloride with the appropriate organocadmium reagents. The latter was prepared in situ by the transmetalation reaction of the corresponding Grignard reagents (neopentyl magnesium chloride and trimethylsilylmethyl magnesium chloride, respectively) with anhydrous cadmium chloride at a low temperature (Scheme 3).^[21] The



Scheme 3. Synthesis of phosphorus-bridged [1]ferrocenophanes **2** and **3**.

known phosphorus-bridged [1]ferrocenophane with a *tert*-butyl substituent on phosphorus (**1**)^[20] and the new analogues with neopentyl (**2**) and (trimethylsilyl)methyl groups (**3**) were synthesized by salt-elimination reactions of $[\text{Fe}(\eta\text{-C}_5\text{H}_4\text{Li})_2] \cdot 2/3 \text{ TMEDA}$ (TMEDA = *N,N,N',N'*-tetramethylethylenediamine) with the appropriate alkylidichlorophos-

phines (RPCl_2) in hexane (Scheme 3). As reported earlier,^[20] column chromatography was required to separate **1** from the yellow phosphorus-bridged [1,1]ferrocenophane byproduct. However, no analogous byproducts were observed during the syntheses of **2** and **3**, as monitored by ^{31}P NMR spectroscopic studies. The phosphorus-bridged [1]ferrocenophanes **2** and **3** were obtained in good yields, as dark-red, moisture and air-sensitive solids. Analytically pure samples of compounds **2** and **3**, suitable for living anionic polymerization, were obtained by successive recrystallizations from hexane and vacuum sublimations.

Compounds **1–3** were characterized by multinuclear NMR spectroscopy, elemental analysis, and mass spectrometry and the data were consistent with the assigned structures of the phosphorus-bridged [1]ferrocenophanes. The solution UV/Vis absorption of monomers **1–3** exhibits typical features of strained ferrocenophanes. The electronic absorption spectra in hexane showed that the intense red color of **1–3** is due to the absorption bands at 494–498 nm, which are significantly redshifted relative to the silicon-bridged [1]ferrocenophanes.^[2a] The $^{31}\text{P}\{^1\text{H}\}$ NMR spectra of **1–3** in C_6D_6 showed singlets at $\delta = 26.1$, -10.8 , and -7.1 ppm, respectively. The ^1H NMR spectra for **1–3** exhibited four separate resonances in the Cp region ($\delta = 4.18$ – 4.45 ppm). The methylene protons for **2** and **3** appeared as doublets at $\delta = 1.95$ and 1.15 ppm, respectively. As observed for other strained and ring-tilted bridged [1]ferrocenophanes, the most distinguishing feature of the ^{13}C NMR spectra for **1–3** (in C_6D_6) is the upfield shift of the *ipso*-carbon atom resonances attached to the bridging P atom ($\delta = 19.4$, 19.6 , and 20.8 ppm, respectively) relative to the other cyclopentadienyl carbon atoms. Mass spectra were consistent with the assigned structures and showed peaks arising from the molecular ions and the loss of alkyl side groups attached to phosphorus. To further characterize the molecular structures of **2** and **3**, dark-red single crystals suitable for X-ray crystallography were grown by vacuum sublimation. The molecular structures of **2** and **3**, obtained from the single crystal X-ray diffraction studies, are shown in Figures 1 and 2, respectively. Two independent molecules of **2** were located in the asymmetric unit with negligible differences in their metrical parameters. The Fe–P distances in **2** are 2.8187(11) and 2.8106(11) Å, which are significantly longer than that of normal Fe–P bonds (ca. 2.40 Å).^[22] The tilt-angles (α , the angle between the planes of the two Cp rings) in the phosphorus-bridged [1]ferrocenophane **2** were found to be 27.30(10) and 27.25(22)° (for the two independent molecules in the asymmetric unit), whereas the average β angle (the angle between each Cp plane and the corresponding P–C_{*ipso*} bond) are 30.97 and 31.20°, similar to that in **1**,^[20] which suggests an appreciable amount of ring strain. The Fe–P distance in **3** was found to be 2.7975(5) Å, which is slightly smaller than that in **2**. The tilt angle α of 27.10(10)° and the average β angle of 32.05° in **3** are comparable to that of **2**. It should be noted that the tilt-angles of the phosphorus-bridged [1]ferrocenophanes are much higher than those of the silicon-bridged [1]ferrocenophanes, which indicates more ring strain associated with the

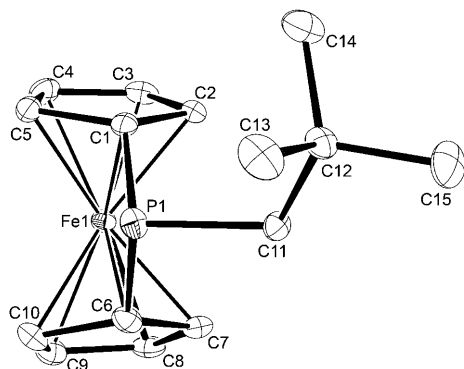
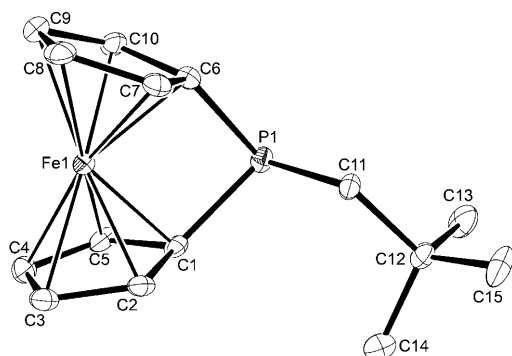


Figure 1. ORTEP diagram (50% probability thermal ellipsoids) of the molecular structure of **2** with important atoms labeled. Hydrogen atoms are omitted for the sake of clarity. Important bond lengths [Å] and angles [°]: Fe1–P1 2.8187(11), P1–C1 1.857(4), P1–C6 1.855(4); C6–P1–C1 89.39(16); distortion parameters [°]: α (ring tilt, the angle between the planes of the two Cp rings) 27.30(10), β (average angle between the plane of the Cp ligand and the C(Cp)–P bond) 30.97, and δ (Cp–Fe–Cp) 158.51.

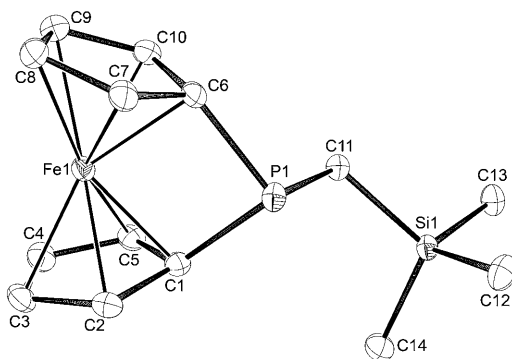
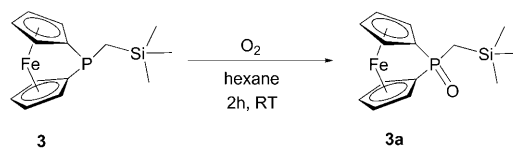


Figure 2. ORTEP diagram (50% probability thermal ellipsoids) of the molecular structure of **3** with important atoms labeled. Hydrogen atoms are omitted for the sake of clarity. Important bond distances [Å] and angles [°]: Fe1–P1 2.7975(5), P1–C1 1.862(2), P1–C6 1.855(2), C6–P1–C1 90.17(8); distortion parameters [°]: α (ring tilt) 27.10(10), β (average angle between the plane of the Cp ligand and the C(Cp)–P bond) 32.05, and δ (Cp–Fe–Cp) 159.56.

former species as a result of the geometric preferences and smaller size of the bridging Group 15 element.

Due to the alkyl substituents on phosphorus, the P^{III} -bridged ferrocenophanes **1–3** are very prone to oxidation by air, yielding the corresponding P^V -bridged [1]ferroceno-

phane oxide. In the case of **3**, the phosphorus(V) species $[Fe\{\eta\text{-}C_5H_4\}_2P(O)(CH_2SiMe_3)]$ (**3a**) was isolated and fully characterized after passing oxygen gas through a hexane solution of **3** (Scheme 4). The species **3a** was characterized by



Scheme 4. Synthesis of phospho[1]ferrocenophane oxide (**3a**).

^{31}P NMR spectroscopy, elemental analysis, mass spectrometry, and by X-ray crystallography. To the best of our knowledge, this represents the first X-ray structure of a phospho[1]ferrocenophane oxide. Two independent molecules of **3a** were located in the asymmetric unit (Figure 3). The Fe–P

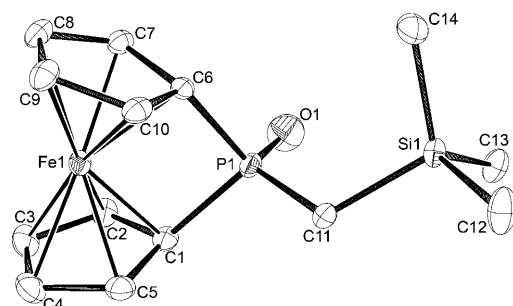


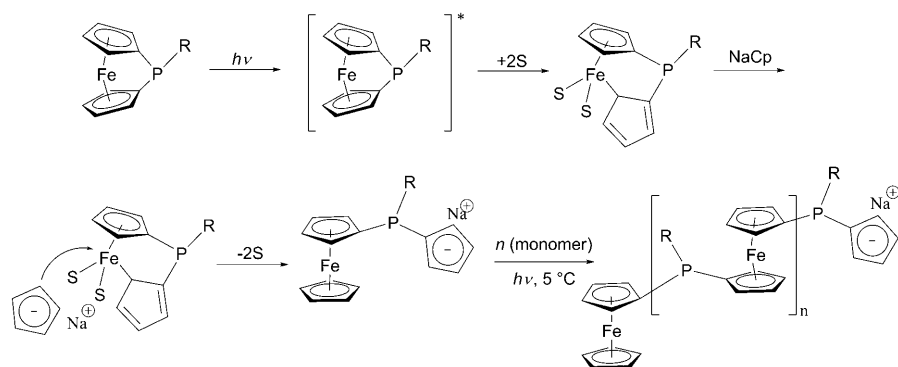
Figure 3. ORTEP diagram (50% probability thermal ellipsoids) of the molecular structure of **3a** with important atoms labeled. Hydrogen atoms are omitted for the sake of clarity. Important bond distances [Å] and angles [°]: Fe1–P1 2.7116(7), P1–C1 1.827(2), P1–C6 1.829(2), P1–O1 1.427(2), C6–P1–C1 94.26(10); distortion parameters: α (ring tilt) 25.36(12), β (average angle between the plane of the Cp ligand and the C(Cp)–P bond) 34.41, and δ (Cp–Fe–Cp) 161.37.

distance is slightly shorter (2.7116(7) and 2.7061(6) Å) in **3a** relative to that observed in **3** providing evidence that the P^V center in **3a** may be acting as a better acceptor of electron density than the P^{III} center in **3**, allowing a significant weak interaction between a vacant orbital on the bridging phosphorus and a filled d orbital of iron.^[14,22a] The tilt-angle in **3a** is slightly smaller (25.36(12) and 25.83(12)°) than in **2** and **3**, which suggests a slight relief of ring strain in the P^V -bridged [1]ferrocenophane **3a** relative to the P^{III} analogue (**3**).

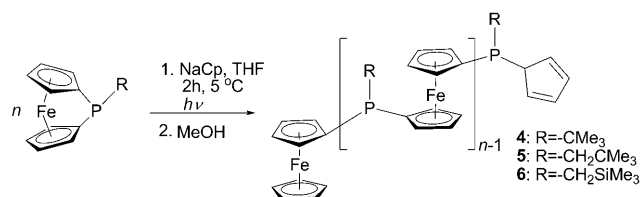
Photocontrolled living anionic ROP of phosphorus-bridged [1]ferrocenophanes 1–3: After successful photocontrolled living anionic ROP of silicon-bridged [1]ferrocenophanes by our group,^[17] we were encouraged to explore this methodology with phosphorus-bridged [1]ferrocenophanes to provide convenient access to well-defined high molecular weight PFPs. Living photolytic anionic ROP of **1–3** in THF was attempted by using $Na[C_5H_5]$ as the initiator (monomer/initiator 50:1) under UV irradiation at 5°C for 2 h (Scheme 5).

The reaction was quenched with a few drops of degassed methanol, affording a yellow PFP homopolymers **4–6** with narrow molecular weight distributions ($M_w/M_n < 1.10$), indicative of a successful living anionic polymerization (Table 1).

The homopolymers obtained by using the above synthetic procedures were characterized by multinuclear NMR spectroscopy and gel-permeation chro-



Scheme 6. Proposed mechanism for photolytic ROP of phosphorus-bridged [1]ferrocenophanes (S = THF).



Scheme 5. Synthesis of PFP homopolymers **4–6** by photocontrolled ROP of the respective monomers initiated by NaCp in THF.

Table 1. Characterization data for PFP homopolymers, **4–6** obtained from the photocontrolled ROP of the respective monomers **1–3** with a monomer/initiator ratio of 50:1.

Polymer	M/I	Yield [%]	M_n [kg mol ⁻¹]		M_w/M_n	T_g [°C]
			Calcd	Exptl ^[a]		
			(Sulfurized)			
4	50:1	91	13.60	15.20	1.09	141
5	50:1	93	14.30	15.90	1.07	127
6	50:1	95	15.11	16.71	1.05	101

[a] Determined by triple detection GPC by using THF as the eluent.

matographic (GPC) analysis. The ³¹P{¹H} NMR spectra (in C₆D₆) confirmed the polymerization of **1–3** by showing single signals at $\delta = -5.2$, -49.9 and -47.1 ppm, respectively, which are shifted to highfield by approximately $\delta = 30$ – 40 ppm relative to that of the respective monomers. The signals for the Cp protons appeared as broad multiplets in the region of $\delta = 4.44$ – 4.20 ppm in the ¹H NMR spectrum. The PCH₂ protons in homopolymers **5** and **6** appeared as broad doublets at $\delta = 2.10$ and 1.42 ppm, respectively. As reported previously, polyferrocenylphosphines do not elute from the GPC column when using THF as the eluent, as they interact with the column material, presumably due to the Lewis basicity of the P^{III} center.^[12,13] For that reason, the polymers with P^{III} sites of polyferrocenylphosphines were sulfurized, resulting in the formation of the corresponding poly(ferrocenylphosphine sulfides), which eluted easily through GPC columns.^[23] The proposed mechanism of the photolytic living anionic ROP of **1–3** is shown in Scheme 6. Whereas the living anionic polymerization of ferrocenophanes by using organolithium initiators proceeds through cleavage of

a phosphorus–cyclopentadienyl (P–Cp) bond in the monomer, photolytic living anionic polymerization proceeds through photoactivation and subsequent cleavage of the iron–cyclopentadienyl (Fe–Cp) bond in the monomer in the presence of the mild nucleophile, Na[C₅H₅]. The monomers **1–3** showed very similar polymerization behavior under photolytic conditions. The polymer chain length could be controlled by the monomer-to-initiator ratio as expected for a living polymerization. To confirm this, the ratio of monomer **2** to initiator was varied from 25:1 to 150:1. This produced well-defined homopolymers **5a–d** with controlled molecular weights and narrow molecular weight distributions as monitored by GPC analysis of the corresponding poly(ferrocenylphosphine sulfides) (Table 2). This is further supported by

Table 2. Photocontrolled living anionic ROP of **2** with a variation of the M/I ratio.

Polymer	M/I	Yield [%]	M_n [kg mol ⁻¹]		PDI (M_w/M_n)
			Calcd	Exptl ^[a]	
			(Sulfurized)		
5a	25:1	93	7.15	7.95	1.05
5b	50:1	95	14.30	15.90	1.07
5c	100:1	94	28.61	31.81	1.14
5d	150:1	95	42.92	47.72	1.23
5e	200:1	91	57.23	63.63	1.40 ^[b]

[a] Molecular weights of the corresponding sulfurized homopolymers determined by triple detection GPC by using THF as the eluent. [b] The broader PDI value is a result of slight column adsorption (see text and Figure S1 in the Supporting Information).

the linear plot of molecular weights versus the ratio of monomer to initiator for the polymer **5** (Figure 4), which indicates the absence of significant chain transfer and chain termination during polymerization. Thus molecular weights of the sulfurized PFP homopolymers could be controlled from $M_n = 11.85 \times 10^3$ to 56.15×10^3 Da with narrow polydispersities (1.05–1.23). However, it was observed that the PDI value increases with increasing monomer to initiator ratio. A significant tailing effect was observed in the case of higher monomer to initiator ratio (200:1) resulting in a higher value of PDI, presumably due to adsorption of the longer PFP chain to the column material (see Figure S1 in the Supporting Information).

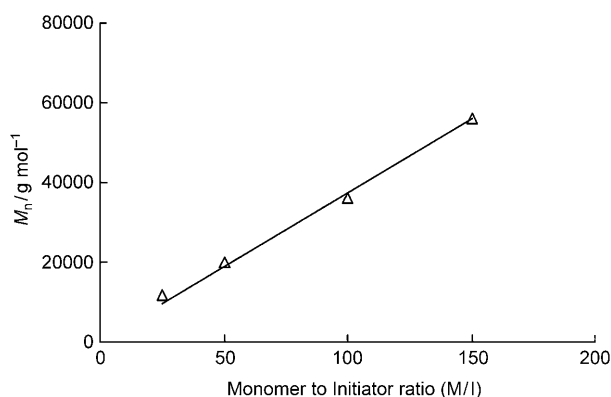
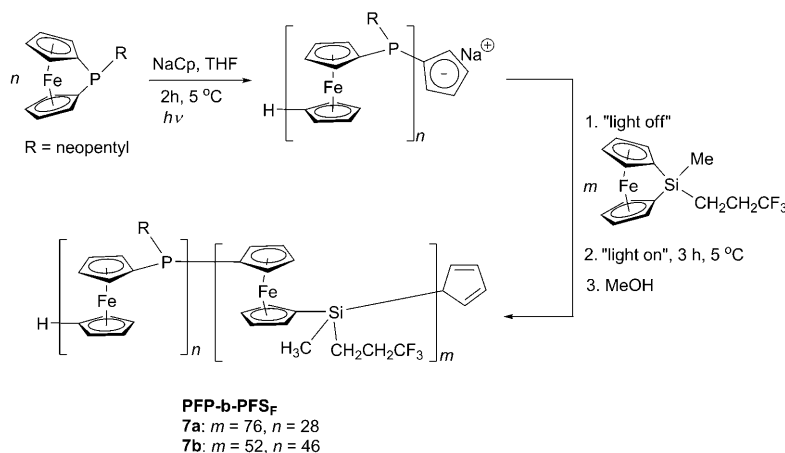


Figure 4. Plot of the molecular weights (M_n) of the homopolymers **5a–d** (after sulfurization of the P^{III} centers) versus monomer to initiator ratio (M:I).

Interestingly, PFP homopolymer **6**, containing a CH_2SiMe_3 substituent on phosphorus, is extremely soluble even in nonpolar solvents, such as *n*-hexane or decane, at ambient temperature. In contrast, the homopolymer **5** is soluble in hot *n*-hexane and decane. All the polymers are very prone to aerial oxidation in solution due to the presence of alkyl groups on the P^{III} centers in the polymer main chain. The homopolymers were found to be considerably more stable to air in the solid state.

Synthesis and characterization of polyferrocenylphosphine-b-polyferrocenylsilane diblock copolymers: The living photocontrolled ROP of phosphorus-bridged [1]ferrocenophanes allows for the sequential polymerization of different monomers to synthesize block copolymers. Thus the polyferrocenylneopentylphosphine-b-polyferrocenylmethyl(3,3,3-trifluoropropyl)silane (PFP-b-PFS_F) block copolymers (**7a** and **7b**) were synthesized by first initiating $[Fe\{\eta-C_5H_4\}_2P(CH_2CMe_3)]$ (**2**) with $Na[C_5H_5]$ and photolyzing for 2 h at 5 °C (Scheme 7).^[24] The color of the solution changed from dark red to orange. The light was switched off and a solution



Scheme 7. Synthesis of diblock copolymers PFP-b-PFS_F (**7a** and **7b**) through sequential photocontrolled anionic ROP.

of monomer $[Fe(\eta-C_5H_4)_2SiMe(CH_2CH_2CF_3)]$ in THF was added to the orange solution. The solution was then irradiated for a further period of 3 h at 5 °C and the polymerization was finally quenched with a few drops of degassed methanol. The block copolymers **7a** and **7b**, with different block ratios, were precipitated into degassed methanol, affording amber solids. The materials were obtained in excellent yields and possessed narrow molecular weight distributions. Shown in Figure 5 are representative GPC traces of a PFP-

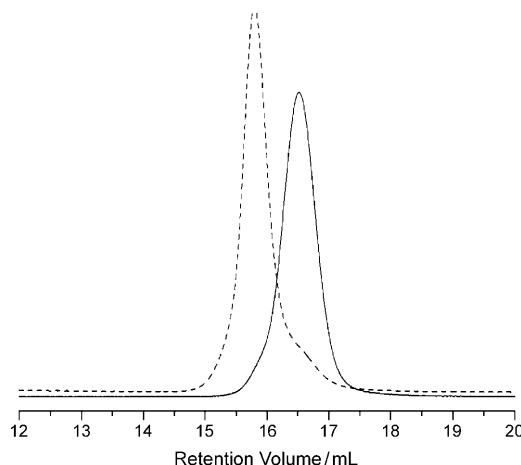


Figure 5. GPC curves (Refractive Index Response) of sulfurized PFP-b-PFS_F diblock copolymer **7b** (----) and the corresponding sulfurized PFP homopolymer (—).

b-PFS_F copolymer (**7b**) and the corresponding PFP homopolymer. A minute amount of PFP homopolymer contaminated with copolymer **7b**, resulting from the quenching of the living PFP chain, was detected in the GPC trace of **7b**. The chemical shifts in the $^{31}P\{^1H\}$, $^{19}F\{^1H\}$, and $^{29}Si\{^1H\}$ NMR spectra of the diblock copolymers (**7a** and **7b**) were similar to those observed for their respective homopolymers. The 1H NMR spectra were used to confirm the structure of the block copolymers. The signals for the Cp protons of the PFP and PFS_F blocks overlapped and appeared as broad multiplets in the region of $\delta = 4.45\text{--}3.85$ ppm. The block ratio in PFP-b-PFS_F copolymers, **7a** and **7b**, was calculated by 1H NMR spectroscopic integration of the SiMe protons of the PFS_F block at $\delta = 0.43$ ppm and the CMe₃ protons of the PFP block at $\delta = 1.18$ ppm. The characteristics of these polymers are presented in Table 3.

Table 3. Characterization data for PFP-b-PFS_F diblock copolymers after sulfurization of the P^{III} centers.

Polymer	PFP block		PFP _n -b-PFS _{Fm}				
	M_n [kg mol ⁻¹] Exptl ^[a]	PDI	M_n [kg mol ⁻¹] Exptl ^[b]	PDI	Yield [%]	n/m ^[c]	ϕ_{PFSF} ^[d]
7a	24.16	1.07	33.25	1.10	88	76:28	0.25
7b	16.55	1.06	31.46	1.05	90	52:46	0.45

[a] Obtained from triple detection GPC of the sulfurized PFP blocks. [b] Determined by combining the M_n of the first block (obtained from GPC) and the block ratio (obtained from ¹H NMR spectroscopy). [c] Obtained from ¹H NMR spectroscopic integration. [d] The volume fraction of PFS_F was calculated by considering the following density values (ρ [g cm⁻³]) for the two blocks: 1.149 (PFP)^[6b,25] and 1.431 (PFS_F)^[6b].

Thermal characterization of PFP homopolymers and diblock copolymers: The thermal transition behavior and thermal stability of the homopolymers **4–6** were analyzed by differential scanning calorimetry (DSC) and thermogravimetric analysis (TGA). All the polymers were found to be thermally stable without weight loss up to 380 °C. DSC analysis suggests that the PFPs (**4–6**) are amorphous as no melting or crystallization temperature was observed from –50 to 250 °C. DSC analysis showed that the glass transition temperature (T_g) of PFPs strongly depends upon the substituents on phosphorus. The high T_g values of the homopolymers **4–6** were found to be 141, 127, and 101 °C, respectively, consistent with the brittle nature of the thin film of the materials at 25 °C (see Table 1 and Figure S2 in the Supporting Information). The highest value of T_g for **4** was anticipated due to the presence of the rigid and bulky *tert*-butyl substituents, which would be expected to hinder large-scale conformational motion. The slightly larger steric requirement of the neopentyl group relative to the CH₂SiMe₃ group explains the higher T_g of **5** relative to that of **6**.

The PFS_F homopolymer has been shown to be amorphous in previous studies.^[26] DSC studies of the PFP-b-PFS_F diblock copolymers show two distinctive endothermic transitions corresponding to the glass transition temperatures (T_g) centered at 60 and 123 °C. The glass transition temperatures obtained were consistent with those of the corresponding homopolymers. The presence of two distinct glass transition temperatures is indicative of the microphase separations of the immiscible PFP and PFS_F blocks in the solid state (vide infra). Figure 6 illustrates the DSC scan for diblock copolymer **7b**.

Thin-film self-assembly studies of the diblock copolymers 7a and 7b: The microphase separation behavior of PFP-b-PFS_F diblock copolymers **7a** and **7b** was studied by TEM in bright field mode. The fluorinated block facilitates segregation behavior by increasing the Flory–Huggins parameter between the two different blocks.^[27] Microphase separation was observed in the thin films of PFP-b-PFS_F diblock copolymers. Fluorine-substituted PFS was anticipated to give darker regions by bright field TEM owing to its greater electron density. As predicted, the diblock copolymer **7a** with a lower volume fraction of PFS_F ($\phi_{\text{PFSF}} = 0.25$) formed a disor-

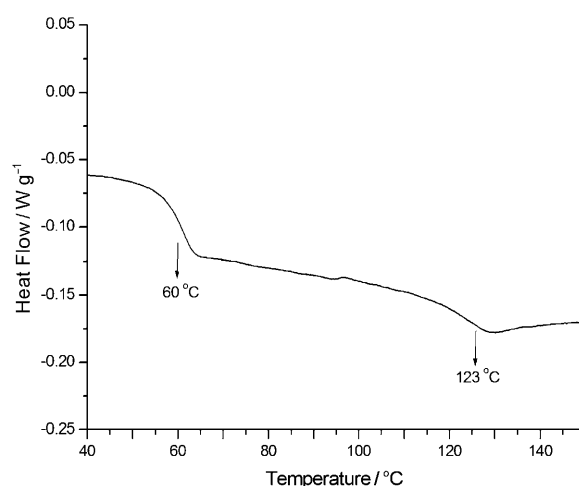


Figure 6. DSC scan for the diblock copolymer **7b** obtained at a scan rate of 10 °C min⁻¹.

dered array of PFS_F spheres (Figure 7A), whereas for **7b** with a relatively higher volume fraction of PFS_F ($\phi_{\text{PFSF}} = 0.45$), an apparent cylindrical morphology was observed (Figure 7B).

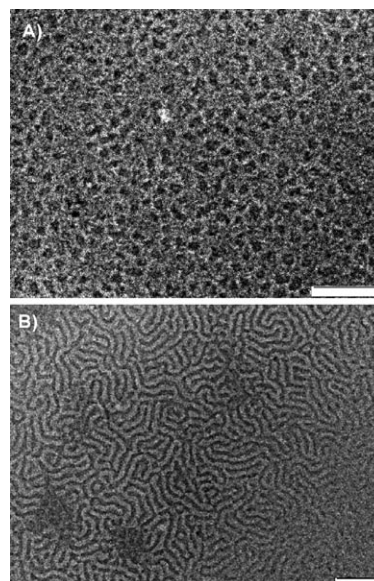


Figure 7. Bright field TEM micrograph of drop-cast thin films showing phase separation of PFP-b-PFS_F block copolymers **7a** (A) and **7b** (B) (scale bar = 200 nm).

Conclusion

We have explored photocontrolled living anionic ROP of the phosphorus-bridged [1]ferrocenophanes [Fe{(η -C₅H₄)₂PR}] (R = alkyl groups, such as CMe₃, CH₂CMe₃, and CH₂SiMe₃) initiated by NaCp in THF at 5 °C, which provides access to well-defined polyferrocenylphosphines [Fe{(η -C₅H₄)₂PR}]_n, with molecular weight control and narrow

polydispersities. Sequential polymerization allows access to well-defined diblock copolymer PFP-*b*-PFS_{*n*}, which undergoes microphase separation in thin films.

We are currently exploring the synthesis and applications of highly metallized polymers, as coordination of metal fragments to the PFP block is possible. In addition, the alkane-soluble PFP blocks with CH₂SiMe₃ permits us to study the solution self-assembly through crystallization-driven living polymerizations, characteristic of crystalline polyferrocenylsilane cores forming blocks.^[9d] The self-assembled PFP-*b*-PFS materials have potential applications in the preparation of functional polymer-metal hybrid nanomaterials and in catalysis. Detailed studies of the self-assembly of PFP-*b*-PFS with these aims in mind are currently underway and the results will be published in the near future.

Experimental Section

Materials and instrumentation: All reactions and manipulations were carried out under an atmosphere of pre-purified N₂ by using standard Schlenk techniques or an inert atmosphere glove box (M-Braun). Solvents were dried by using anhydrous engineering double alumina and alumina/copper catalyst drying columns or by conventional methods.^[28] THF was distilled from Na/benzophenone under reduced pressure prior each photolytic polymerization reaction. Methanol, used for quenching the polymerization, was deoxygenated with considerable care by the freeze-and-thaw technique. Oxygen of purity level above 99.5% was used for the oxidation of **3**. All chemicals were purchased from Aldrich unless otherwise noted. Neopentyl chloride was acquired from ABCR. PCl₃ was distilled prior to use. Dilithioferrocene-2/3 TMEDA,^[29] [Fe(η-C₅H₄)₂PCMe₃] (**1**)^[20] and [Fe{(η-C₅H₄)₂SiMe(CH₂CH₂CF₃)}]^[26a] were synthesized according to the previously reported literature procedures. Photoirradiation experiments were carried out by using Pyrex-glass-filtered emission (λ > 310 nm) from a 125 W high pressure Hg arc lamp (Photochemical Reactors Ltd).

¹H (300 MHz), ¹³C{¹H} (75.6 MHz), ³¹P{¹H} (121.4 MHz), and ¹⁹F{¹H} NMR (282.7 MHz) spectra were obtained from a JEOL Lambda 300 spectrometer. Spectra were internally referenced to residual solvent peaks (¹H, ¹³C) or externally referenced to H₃PO₄ (³¹P) and CFCl₃ (¹⁹F). Mass spectra were obtained by the use of a VG Analytical Autospec mass spectrometer operating in electron impact (EI) mode. Electronic absorptions were measured on a Lambda 35 spectrophotometer employing standard quartz cells (1 cm) from 200 to 800 nm. Elemental analyses were performed by using a Eurovector EA3000 CHN analyzer. Gel-permeation chromatography (GPC) was carried out by using a Viscotek VE 2001 triple detector gel-permeation chromatograph, equipped with an automatic sampler, a pump, an injector, an inline degasser, and a column oven (30 °C). The elution columns consist of styrene divinyl benzene gel with pore sizes of 500 and 100 000 Å. Detection was conducted by means of a VE 3580 refractometer, a four capillary differential viscometer, and a 90° and low-angle (7°) laser light (λ₀ = 670 nm) scattering detector, VE 3210 and VE 270. THF (purchased from Fisher) was used as the eluent, with a flow rate of 1.0 mL min⁻¹. DSC analyses were performed on a Q100 from TA instruments coupled to a refrigerated cooling system (RCS90). The samples, placed in nonhermetic aluminum pans, were tared with a XT220A Precisa microbalance. Copper grids from Agar Scientific (mesh 400) were coated with carbon film. TEM was performed on Jeol 1200EX TEM Mk2, which operates with a tungsten filament operating at 120 kV. It is fitted with a MegaViewII digital camera, by using Soft Imaging Systems GmbH analySIS 3.0 image analysis software.

Synthesis of neopentyl dichlorophosphine: A solution of neopentyl chloride (10.0 g, 93.80 mmol) in diethylether (150 mL) was added through a cannula to magnesium turnings (2.28 g, 93.80 mmol), which had been acti-

vated by grinding and stirring in a vacuum for 4 h. After the addition of half of the solution, 1,2-dibromoethane (0.1 mL) was added to the reaction mixture and was heated to reflux. When the reaction mixture started to become turbid, the remaining solution of neopentyl chloride was added. Stirring was continued at reflux temperature for 12 h after which time a colorless suspension was obtained. The suspension of neopentyl magnesium chloride was separated from the unreacted Mg by transferring through a cannula to a Schlenk flask. The solution of neopentyl magnesium chloride was cooled in an ice bath and stirred vigorously whilst powdered anhydrous CdCl₂ (8.62 g, 46.91 mmol) was added rapidly. After stirring for 2 h at 0 °C, the salt was removed by filtration under a positive pressure of N₂. The filtrate was added over 30 min to a vigorously stirred solution of PCl₃ (38.65 g, 24.60 mL, 281.43 mmol) in anhydrous Et₂O (100 mL). After the addition was complete, the mixture was stirred at room temperature for 3 h. The white precipitate was filtered off, the filter cake was washed with Et₂O, and the combined Et₂O solution was evaporated to get an oily colorless product that was sufficiently pure (95% according to ³¹P NMR spectroscopy) for the next step. Yield: 9.7 g (60%); ¹H NMR (300.4 MHz, C₆D₆, 25 °C): δ = 2.44 (d, 2H; PCH₂), 1.06 ppm (s, 9H; CMe₃); ¹³C{¹H} NMR (75.6 MHz, C₆D₆, 25 °C): δ = 38.2 (d; PCH₂), 31.2 ppm (s; CMe₃); ³¹P{¹H} NMR (121.4 MHz, C₆D₆, 25 °C): δ = 198.9 ppm (s).

Synthesis of (trimethylsilyl)methyl dichlorophosphine: (Trimethylsilyl)methyl dichlorophosphine was prepared by following a similar procedure to that described for the synthesis of neopentyl dichlorophosphine, with (trimethylsilyl)methyl magnesium chloride (60 mL, 60.0 mmol, 1 M solution in diethyl ether), powdered anhydrous CdCl₂ (5.50 g, 30.0 mmol), and PCl₃ (24.72 g, 15.7 mL, 180.0 mol). Yield: 8.1 g (71%); ¹H NMR (300.4 MHz, C₆D₆, 25 °C): δ = 1.92 (d, 2H; PCH₂), 0.09 ppm (s, 9H; SiMe₃); ¹³C{¹H} NMR (75.6 MHz, C₆D₆, 25 °C): δ = 10.2 (d; PCH₂), 0.1 ppm (s; SiMe₃); ³¹P{¹H} NMR (121.4 MHz, C₆D₆, 25 °C): δ = 205.8 ppm (s).

Synthesis of [Fe{(η-C₅H₄)₂P(CMe₃)}] (1**):** This procedure was adapted from that previously reported.^[20] A solution of *tert*-butyl dichlorophosphine (8.40 g, 52.83 mmol) in hexanes (100 mL) was added slowly over a period of 15 min to a stirred suspension of dilithioferrocene-2/3 TMEDA (14.20 g, 51.57 mmol) in hexane (200 mL) at -30 °C. The reaction mixture was then allowed to warm to room temperature and was stirred for another 6 h. The resulting red suspension was filtered to remove LiCl. The solvent and TMEDA were then removed under vacuum. The red residue was dissolved in hexane (50 mL) and the solution was introduced onto a 15 cm × 5 cm column of neutral silica. A mixture of 1:5 v/v toluene and hexane was used as the eluent to separate the red-colored [Fe{(η-C₅H₄)₂P(CMe₃)}] from a yellow phosphine byproduct. The ferrocenophane was crystallized from hexanes at -65 °C twice resulting in dark-red colored needles of [Fe{(η-C₅H₄)₂P(CMe₃)}] (**1**) monomer suitable for photocontrolled living anionic polymerization. Yield: 3.85 g (28%); ¹H NMR (300.4 MHz, C₆D₆): δ = 4.45 (m, 2H; Cp), 4.37 (m, 2H; Cp), 4.23 (m, 2H; Cp), 4.22 (m, 2H; Cp), 1.25 ppm (s, 9H; CMe₃); ¹³C{¹H} NMR (75.6 MHz, C₆D₆): δ = 78.4–72.1 (Cp), 30.2 (s; CMe₃), 19.4 ppm (d; *ipso*-C); ³¹P{¹H} NMR (121.4 MHz, C₆D₆): δ = 26.1 ppm (s); MS (EI, 70 meV): *m/z* (%): 272 (100) [*M*]⁺, 215 (65) [*M* - CMe₃]; elemental analysis calcd (%) for C₁₄H₁₇FeP: C 61.80, H 6.30; found: C 61.92, H 6.41; UV/Vis (hexane): λ (ε) = 495 (438 m⁻¹ cm⁻¹), 412 nm (shoulder).

Synthesis of [Fe{(η-C₅H₄)₂P(CH₂CMe₃)}] (2**):** A solution of neopentyl dichlorophosphine (5.40 g, 31.21 mmol) in hexanes (100 mL) was added slowly over a period of 15 min to a stirred suspension of dilithioferrocene-2/3 TMEDA (8.60 g, 31.23 mmol) in hexanes (150 mL) at -30 °C. The reaction mixture was then allowed to warm to room temperature and stirred for another 6 h. The resulting red suspension was filtered to remove LiCl. The solvent and TMEDA were then removed under vacuum. The ferrocenophane was crystallized from hexanes at -65 °C and further purified by sublimation (70 °C, 0.005 mm Hg) resulting in a dark-red colored crystalline ferrocenophane monomer suitable for photocontrolled living anionic polymerization. Yield: 6.10 g (68%); ¹H NMR (300.4 MHz, C₆D₆): δ = 4.40 (m, 2H; Cp), 4.31 (m, 2H; Cp), 4.25 (m, 2H; Cp), 4.18 (m, 2H; Cp), 1.95 (d, 2H; PCH₂), 1.12 ppm (s, 9H; CMe₃);

$^{13}\text{C}\{^1\text{H}\}$ NMR (75.6 MHz, C_6D_6): δ = 78.8–72.5 (Cp), 39.4 (d; PCH_2), 31.2 (s; CMe_3), 19.6 ppm (d; *ipso*-C); $^{31}\text{P}\{^1\text{H}\}$ NMR (121.4 MHz, C_6D_6): δ = –10.8 ppm (s); MS (EI, 70 meV): m/z (%): 286 (100) [M^+], 230 (60) [$\text{M}^+ - \text{CMe}_3$]; elemental analysis calcd (%) for $\text{C}_{15}\text{H}_{19}\text{FeP}$: C 62.96, H 6.69; found: C 63.55, H 6.43; UV/Vis (hexane): λ (ϵ) = 497 (548 $\text{m}^{-1}\text{cm}^{-1}$), 414 nm (shoulder).

Synthesis of $[\text{Fe}(\eta\text{-C}_5\text{H}_4)_2\text{P}(\text{CH}_2\text{SiMe}_3)]$ (3**):** Compound **3** was synthesized by following the procedures similar to that described for **2**. A solution of (trimethylsilyl)methyl dichlorophosphine (7.83 g, 41.41 mmol) in hexanes (100 mL) was added slowly over a period of 15 min to a stirred suspension of dilithioferrocene-2/3TMEDA (11.40 g, 41.40 mmol) in hexanes (150 mL) at -30°C . The reaction mixture was then allowed to warm to room temperature and was then stirred for another 6 h. The resulting red suspension was filtered to remove LiCl. The solvent and TMEDA were removed under vacuum. The ferrocenophane was crystallized from hexanes twice at -65°C and further purified by sublimation (70°C , 0.005 mmHg) to obtain a dark-red-colored crystalline compound, **3**, suitable for photocontrolled living anionic polymerization. Yield 8.12 g (65%); ^1H NMR (300.4 MHz, C_6D_6): δ = 4.42 (m, 2H; Cp), 4.35 (m, 2H; Cp), 4.29 (m, 2H; Cp), 4.22 (m, 2H; Cp), 1.15 (d, 2H; PCH_2), 0.20 ppm (s, 9H; SiMe_3); $^{13}\text{C}\{^1\text{H}\}$ NMR (75.6 MHz, C_6D_6): δ = 78.1–74.2 (Cp), 20.8 (d; *ipso*-C), 10.1 (d; PCH_2), –0.1 ppm (brs, SiMe_3); $^{31}\text{P}\{^1\text{H}\}$ NMR (121.4 MHz, C_6D_6): δ = –7.1 ppm (s); MS (EI, 70 meV): m/z (%): 302 (100) [M^+], 230 (40) [$\text{M}^+ - \text{SiMe}_3$]; elemental analysis calcd (%) for $\text{C}_{14}\text{H}_{19}\text{FePSi}$: C 55.64, H 6.34; found: C 56.38 H 6.36; UV/Vis (hexane): λ (ϵ) = 498 (465 $\text{m}^{-1}\text{cm}^{-1}$), 413 nm (shoulder).

Synthesis of $[\text{Fe}(\eta\text{-C}_5\text{H}_4)_2\text{P}(\text{O})(\text{CH}_2\text{SiMe}_3)]$ (3a**):** Compound **3** (50 mg, 0.165 mmol) was dissolved in dry hexanes (5 mL) in a Schlenk tube and dry oxygen gas (>99.5% purity) was bubbled into the solution for 2 h at ambient temperature. The solution was kept at -30°C for 2 days to give red-orange crystals of $[\text{Fe}(\eta\text{-C}_5\text{H}_4)_2\text{P}(\text{O})(\text{CH}_2\text{SiMe}_3)]$. Yield 32 mg (60%); ^1H NMR (300.4 MHz, C_6D_6): δ = 4.44 (s, 2H; Cp), 4.36 (s, 2H; Cp), 4.29 (s, 2H; Cp), 4.21 (s, 2H; Cp), 1.18 (d, 2H; PCH_2), 0.22 ppm (s, 9H; SiMe_3); $^{13}\text{C}\{^1\text{H}\}$ NMR (75.6 MHz, C_6D_6): δ = 78.2–74.2 (Cp), 21.7 (d; *ipso*-C), 11.0 (d; PCH_2), –0.1 ppm (brs, SiMe_3); $^{31}\text{P}\{^1\text{H}\}$ NMR (121.4 MHz, C_6D_6): δ = 32.2 ppm (s); MS (EI, 70 meV): m/z (%): 318 (65) [M^+]; elemental analysis calcd (%) for $\text{C}_{14}\text{H}_{19}\text{FeOPSi}$: C 52.84, H 6.02; found: C 51.41, H 6.14; UV/Vis (dichloromethane): λ (ϵ) = 482 nm (361 $\text{m}^{-1}\text{cm}^{-1}$).

Synthesis of PFP homopolymers (4–6**):** A representative photolytic homopolymerization of **2** to yield **5b** is described. In the absence of light, the monomer **2** (45 mg, 0.157 mmol) was dissolved in dry THF (1 mL) in a Schlenk tube. $\text{Na}[\text{C}_5\text{H}_5]$ (37 μL , 3.14×10^{-3} mmol, 0.085 M solution in THF) was added and the mixture was photolyzed to initiate the polymerization. The reaction was maintained at 5°C with stirring for 2 h by using a thermostatically controlled water bath. The color of the solution changed from a dark red to light orange. The polymerization was quenched with a few drops of degassed methanol. Precipitation of the solution into rapidly stirred degassed methanol (20 mL) followed by drying overnight under vacuum afforded polymer **5b** as a yellow powder. Homopolymers **4** and **6** were synthesized by following procedures similar to that described for **5b**.

PFP homopolymer 4: ^1H NMR (300.4 MHz, C_6D_6): δ = 4.44–4.21 (brm, 8H; Cp), 1.26 ppm (brs, 9H; CMe_3); $^{13}\text{C}\{^1\text{H}\}$ NMR (75.6 MHz, C_6D_6): δ = 78.7–72.45 (Cp), 30.1 (s; CMe_3); $^{31}\text{P}\{^1\text{H}\}$ NMR (121.4 MHz, C_6D_6): δ = –5.2 ppm (s).

PFP homopolymer 5: ^1H NMR (300.4 MHz, C_6D_6): δ = 4.40–4.23 (brm, 8H; Cp), 2.10 (brd, 2H; PCH_2), 1.21 ppm (s, 9H; CMe_3); $^{13}\text{C}\{^1\text{H}\}$ NMR (75.6 MHz, C_6D_6 , 25°C): δ = 78.7–72.4 (Cp), 39.4 (d, PCH_2), 31.2 ppm (s, CMe_3); $^{31}\text{P}\{^1\text{H}\}$ NMR (121.4 MHz, C_6D_6): δ = –49.9 ppm (s).

PFP homopolymer 6: ^1H NMR (300.4 MHz, C_6D_6 , 25°C): δ = 4.39–4.20 (brm, 8H; Cp), 1.42 (brd, 2H; PCH_2), 0.22 ppm (s, 9H; SiCH_3); $^{13}\text{C}\{^1\text{H}\}$ NMR (75.6 MHz, C_6D_6 , 25°C): 77.6–76.5 (brs, Cp), 10.1 (brd, PCH_2), –0.15 ppm (brs, SiCH_3); $^{31}\text{P}\{^1\text{H}\}$ NMR (121.4 MHz, C_6D_6): δ = –47.1 ppm (s).

The yields and the characterization data including GPC analyses for **4–6** are tabulated in Table 1.

Synthesis of PFP-*b*-PFS_F diblock copolymers (7a** and **7b**):** A representative diblock copolymerization to yield **7b** is described. Monomer $[\text{Fe}(\eta\text{-C}_5\text{H}_4)_2\text{P}(\text{CH}_2\text{CMe}_3)]$ (289 mg, 1.01 mmol) was dissolved in dry THF (1 mL) in a Schlenk tube in the absence of light. A solution of $\text{Na}[\text{C}_5\text{H}_5]$ (0.1 M, 200 μL , 0.02 mmol) was added to that and the reaction mixture was irradiated at 5°C with stirring for 2 h. The color of the solution changed from dark red to light orange. The Schlenk tube was brought into the glovebox, a sample of the solution (0.1 mL) was withdrawn to characterize the homopolymer by GPC. A solution of $[\text{Fe}(\eta\text{-C}_5\text{H}_4)_2\text{SiMe}(\text{CH}_2\text{CH}_2\text{CF}_3)]$ (250 mg, 0.77 mmol) in dry THF (1 mL) was added to the remainder of the solution. The solution was then photolyzed for a further 3 h at 5°C with stirring. The reaction was quenched with a few drops of degassed methanol, and the solution was precipitated into degassed methanol (30 mL). The block copolymer was further purified by repetitive precipitation in methanol and finally washed with warm hexanes to remove the minute amount of PFP homopolymer contaminated with the block copolymer. The block copolymer **7b** was obtained as a yellow solid and dried under vacuum. Yield: (460 mg, 90%).

Diblock copolymer 7b: ^1H NMR (300.4 MHz, C_6D_6): δ = 4.42–3.87 (brm; Cp), 2.18 (brm, 2H; $\text{SiCH}_2\text{CH}_2\text{CF}_3$), 2.12 (brd, 2H; PCH_2), 1.22 (brm, 2H; $\text{SiCH}_2\text{CH}_2\text{CF}_3$), 1.18 (s; $-\text{CMe}_3$), 0.43 ppm (brs; SiCH_3); $^{13}\text{C}\{^1\text{H}\}$ NMR (75.6 MHz, C_6D_6): δ = 131.2 (CF_3), 79.7–69.8 (Cp), 39.5 (d, PCH_2), 31.1 (s, CMe_3), 29.7 ($\text{SiCH}_2\text{CH}_2\text{CF}_3$), 8.8 ($\text{SiCH}_2\text{CH}_2\text{CF}_3$), –3.3 ppm (Si-CH_3); $^{31}\text{P}\{^1\text{H}\}$ NMR (121.4 MHz, C_6D_6): δ = –49.9 ppm (s); ^{19}F NMR (282.6 MHz, C_6D_6): δ = –67.8 ppm; ^{29}Si NMR (59.5 MHz, C_6D_6): δ = –4.5 ppm.

The GPC analyses for the diblock copolymers (after sulfurization) are compiled in Table 3.

Reaction of the polyferrocenylphosphine homopolymers and block copolymers with elemental sulfur to yield the corresponding poly(ferrocenylphosphine sulfides): A representative sulfurization of **4** is described. Homopolymer **4** (30 mg) was dissolved in dichloromethane (2 mL) with stirring. Elemental sulfur (5 mg of S_8) was added to that solution. The reaction mixture was allowed to stir for 12 h. No visual color change was observed. The solution was then filtered and the solvent was removed under vacuum to get a quantitative yield of poly(ferrocenylphosphine sulfides). The ^1H and $^{13}\text{C}\{^1\text{H}\}$ NMR data for the poly(ferrocenylphosphine sulfides) were similar to that of their corresponding parent polyferrocenylphosphines. $^{31}\text{P}\{^1\text{H}\}$ chemical shifts of the poly(ferrocenylphosphine sulfides) obtained from their respective polyferrocenylphosphines (**4–6**) were found to be δ = 59.2, 31.4, and 35.4 ppm. For full characterization, see the Supporting Information and Table 1.

Preparation of PFP-*b*-PFS thin films: Thin films of the diblock copolymers (**7a** and **7b**) were prepared by placing a drop of PFP-*b*-PFS_F solution (10 mg mL^{-1} in THF) on a carbon coated copper grid placed on a piece of filter paper. The samples were then allowed to dry for 12 h under a dry nitrogen atmosphere to avoid aerial oxidation before TEM studies.

X-ray data collections and refinement: The dark-red-colored single crystals of **2** and **3**, suitable for X-ray crystallography, were obtained by vacuum sublimation (60°C , 0.005 mmHg). The orange colored single crystals of **3a** were harvested from a hexane solution at -30°C . Single-crystal X-ray structural studies were performed on a CCD Bruker SMART APEX diffractometer equipped with an Oxford Instruments low-temperature attachment. Data were collected at 100(2) K by using graphite-monochromated MoK_α radiation (λ_α = 0.71073 Å). The frames were indexed, integrated, and scaled by using the SMART and SAINT software package,^[30] and the data were corrected for absorption by using the SADABS program.^[31] Pertinent crystallographic data for **2**, **3**, and **3a** are summarized in Table 4. CCDC-751639, 751640, and -751641 contain the supplementary crystallographic data for this paper. These data can be obtained free of charge from The Cambridge Crystallographic Data Centre via www.ccdc.cam.ac.uk/data_request/cif. The structure was solved and refined by using the SHELX suite of programs.^[32] All molecular structures were generated by using ORTEP-3 for Windows Version 2.02.^[33] The hydrogen atoms were included in geometrically calculated positions in the final stages of the refinement and were refined according

- 2006, 118, 3154; *Angew. Chem. Int. Ed.* **2006**, 45, 3083; g) H. C. Su, O. Fadhel, C. J. Yang, T. Y. Cho, C. Fave, M. Hissler, C. C. Wu, R. Réau, *J. Am. Chem. Soc.* **2006**, 128, 983; h) L. A. Vanderark, T. J. Clark, E. Rivard, I. Manners, J. C. Slootweg, K. Lammertsma, *Chem. Commun.* **2006**, 3332; i) K. Naka, T. Umeyama, A. Nakahashi, Y. Chujo, *Macromolecules* **2007**, 40, 4854; j) K. J. T. Noonan, B. H. Gillon, V. Cappello, D. P. Gates, *J. Am. Chem. Soc.* **2008**, 130, 12876; k) B. H. Gillon, B. O. Patrick, D. P. Gates, *Chem. Commun.* **2008**, 2161; l) A. P. Soto, I. Manners, *Macromolecules* **2009**, 42, 40.
- [11] a) T. J. Peckham, J. A. Massey, C. H. Honeyman, I. Manners, *Macromolecules* **1999**, 32, 2830; b) L. Cao, I. Manners, M. A. Winnik, *Macromolecules* **2001**, 34, 3353.
- [12] D. Seyferth, H. P. Withers, *Organometallics* **1982**, 1, 1275.
- [13] C. H. Honeyman, D. A. Foucher, F. Y. Dahmen, R. Rulkens, A. J. Lough, I. Manners, *Organometallics* **1995**, 14, 5503.
- [14] a) C. E. B. Evans, A. J. Lough, H. Grondley, I. Manners, *New J. Chem.* **2000**, 24, 447; b) K. Temple, F. Jäkle, J. B. Sheridan, I. Manners, *J. Am. Chem. Soc.* **2001**, 123, 1355.
- [15] T. Mizuta, M. Onishi, K. Miyoshi, *Organometallics* **2000**, 19, 5005.
- [16] T. Mizuta, Y. Imamura, K. Miyoshi, *J. Am. Chem. Soc.* **2003**, 125, 2068.
- [17] a) M. Tanabe, I. Manners, *J. Am. Chem. Soc.* **2004**, 126, 11434; b) M. Tanabe, G. W. M. Vandermeulen, W. Y. Chan, P. W. Cyr, L. Vanderark, D. A. Rider, I. Manners, *Nat. Mater.* **2006**, 5, 467.
- [18] D. E. Herbert, U. F. J. Mayer, J. B. Gilroy, M. J. López-Gómez, A. J. Lough, J. P. H. Charmant, I. Manners, *Chem. Eur. J.* **2009**, 15, 12234.
- [19] A. G. Osborne, R. H. Whiteley, R. E. Meads, *J. Organomet. Chem.* **1980**, 193, 345.
- [20] I. R. Butler, W. R. Cullen, F. W. B. Einstein, S. J. Rettig, A. J. Willis, *Organometallics* **1983**, 2, 128.
- [21] S. Amberg, J. W. Engels, *Helv. Chim. Acta.* **2002**, 85, 2503.
- [22] a) T. Mizuta, T. Yamasaki, H. Nakazawa, K. Miyoshi, *Organometallics* **1996**, 15, 1093; b) A. Houlton, R. M. G. Roberts, J. Silver, M. G. B. Drew, *J. Chem. Soc. Dalton Trans.* **1990**, 1543.
- [23] We have previously demonstrated that poly(ferrocenylphosphine sulfides) provide accurate estimates of the molecular weight of their parent PFP polymers, by using GPC with THF as the elution solvent. See references [11a,13].
- [24] It was observed that the PFP-b-PFS block copolymer could also be synthesized by starting from PFS as the first block. The synthetic protocol by starting from PFP is more advantageous as the minute amount of homopolymer resulting from the quenching of the living PFP chain can be washed away with warm hexanes.
- [25] The density (ρ) of the $[\text{Fe}\{(\eta\text{-C}_5\text{H}_4)_2\text{P}(\text{CH}_2\text{CMe}_3)\}]_n$ (with a CH_2CMe_3 group on phosphorus) repeat unit was calculated by using the relationship $\rho = M_{\text{M}}/V_{\text{M}}$ (M_{M} =molar mass and V_{M} =molar volume) and $V_{\text{M}}/V_{\text{W}}=1.60$ (V_{W} =van der Waals volume). The V_{W} value of PFP (with a CH_2CMe_3 group on phosphorus) was calculated by subtracting the V_{W} of a phenyl group from the V_{W} value of the polyferrocenylphenylphosphine ($[\text{Fe}\{(\eta\text{-C}_5\text{H}_4)_2\text{PPh}\}]_n$) repeating unit ($V_{\text{M}}=213\text{ cm}^3\text{ mol}^{-1}$; see: reference [6b]) and subsequently adding the V_{W} value of the CH_2CMe_3 group (tabulated by Van Krevelen) following the reference: D. W. Van Krevelen, *Properties of Polymers*, 3rd ed., Elsevier, Amsterdam, **1990**.
- [26] a) D. Foucher, R. Ziembinski, R. Petersen, J. Pudelski, M. Edwards, Y. Ni, J. Massey, R. Jaeger, G. J. Vancso, I. Manners, *Macromolecules* **1994**, 27, 3992; b) G. S. Smith, S. K. Patra, L. Vanderark, S. Saitong, J. P. Charmant, I. Manners, *Macromol. Chem. Phys.* **2010**, 211, 303.
- [27] D. A. Davidock, M. A. Hillmyer, T. P. Lodge, *Macromolecules* **2004**, 37, 397.
- [28] D. D. Perrin, W. L. F. Armarego, D. R. Perrin, *Purification of Laboratory Chemicals*, 2nd ed., Pergamon Press, New York, **1980**.
- [29] M. S. Wrighton, M. C. Palazzotto, A. B. Bocarsly, J. M. Bolts, A. B. Fischer, L. Nadjo, *J. Am. Chem. Soc.* **1978**, 100, 7264.
- [30] SAINT+ Software for CCD diffractometers, Bruker AXS, Madison, WI, **2000**.
- [31] G. M. Sheldrick, SADABS Program for Correction of Area Detector Data, University of Göttingen, Göttingen, **1999**.
- [32] a) SHELXTL Package, version 6.10, Bruker AXS, Madison, WI, **2000**; b) G. M. Sheldrick, SHELXS-86 and SHELXL-97, University of Göttingen, Göttingen, **1997**.
- [33] L. J. Farrugia, *J. Appl. Crystallogr.* **1997**, 30, 565.

Received: October 19, 2009
Published online: February 16, 2010